Spin filtering and spin Hall accumulation in an interferometric ballistic nanojunction with Rashba spin-orbit interaction

S. Bellucci[1] and P. Onorato[1,2]
[1]*INFN, Laboratori Nazionali di Frascati, P.O. Box 13, 00044 Frascati, Italy*
[2]*Dipartimento di Ingegneria dell'Informazione, Seconda Università di Napoli, 81031 Aversa (CE), Italy*
(Received 23 October 2007; revised manuscript received 4 January 2008; published 5 February 2008)

We propose an all-electrical nanostructure where a spin accumulation, an observable signature of the spin Hall effect, and a spin current are induced in the probes attached to a quantum-coherent ballistic one-dimensional T junction when unpolarized charge current is injected through its longitudinal lead. Our proposal is essentially based on the Rashba spin-orbit interaction (SOI) and on the presence of one lead where the SOI vanishes. Tuning of the Rashba SOI in the semiconductor heterostructure hosting the junction generates quasiperiodic oscillations of the predicted spin current due to spin-sensitive quantum-interference effects caused by the difference in the interferometric phase accumulated by opposite spin states.

DOI: 10.1103/PhysRevB.77.075303 PACS number(s): 72.25.−b, 72.20.My, 73.50.Jt

I. INTRODUCTION

Conventional electronic devices rely on the transport of electrical charge carriers. In recent years, the study of spintronics devices, which utilize the spin rather than the charge of an electron, has been intensified mainly because they are expected to operate at much higher speeds than the conventional ones and have potential applications in quantum computing.[1,2] Among these studies many are focused on the role of the spin-orbit interaction (SOI) in condensed matter systems. The latter interaction is due to the Pauli coupling between the spin momentum of an electron and a magnetic field, which appears in the rest frame of the electron, due to its motion in the electric field[3]

$$\hat{H}_{SO} = -\frac{\lambda_0^2}{\hbar} m_0 e \mathbf{E}(\mathbf{r})[\hat{\sigma} \times \hat{\mathbf{p}}]. \tag{1}$$

Here, m_0 is the electron mass in vacuum, $\hat{\sigma}$ are Pauli matrices, $\hat{\mathbf{p}}$ is the canonical momentum operator, $\mathbf{r}$ is a three-dimensional position vector, and $\lambda_0^2 = \hbar^2/(2m_0c)^2$. In condensed matter systems, m_0 and λ_0 are substituted by their effective values m^* and λ. Thus, many of the proposed spintronics devices are low-dimensional nanostructures that work in the presence of the SOI.

Moreover, several fundamental quantum phenomena, which involve electron spin, have been investigated in order to generate and measure *pure spin currents*, i.e., not accompanied by any net charge current. In contrast to conventional charge currents, or spin-polarized charge currents that have been explored and utilized in metal spintronics over the past two decades,[4] pure spin currents emerge when equal numbers of spin-↑ and spin-↓ electrons move in opposite directions so that the net charge current is zero.[5] A recent theoretical analysis has found potential sources of such currents in the typical devices supporting the so called *spin Hall effect*[6–9] (SHE). The electrical Hall effect[10] manifests itself when an electric current flows along a conductor subject to a perpendicular magnetic field and the Lorenz force deflects the charge carriers, creating a transverse Hall voltage between the lateral edges of the sample.

In analogy to the conventional Hall effect, an external electric field can be expected to induce a pure transverse spin current in the absence of applied magnetic fields. Thus, the SHE is the creation of a spin imbalance, or spin current, due to scattering of electron spin moments in a direction perpendicular to an applied electric field. It follows that the SHE induces edge spin accumulation and a pure spin Hall current flowing in the direction orthogonal both to the electric field and to the injected unpolarized charge current.

Early theoretical studies predicted the SHE as an *extrinsic* effect due to impurities in the presence of SO coupling.[6] When the scattering due to the impurities is spin dependent, spin-↑ and spin-↓ electrons of an unpolarized beam are scattered into opposite directions, resulting in spin-up and spin-down charge Hall currents. It was realized long ago that the extrinsic spin Hall current is the sum of two contributions.[11] The first contribution (commonly known as "skew-scattering" mechanism[12,13]) arises from the asymmetry of the electron-impurity scattering in the presence of spin-orbit interactions,[14] and the second one, i.e., the so-called "side-jump" mechanism,[11,15–17] is caused by the anomalous relationship between the physical and the canonical position operator.[18]

More recently, it has been pointed out that there may exist a different SHE purely *intrinsic*. A pure transverse spin Hall current should be observed, that is, several orders of magnitude larger than in the case of the extrinsic effect, arising due to intrinsic mechanisms related to the spin-split band structure in SO coupled bulk[19,20] or mesoscopic[21] semiconductor systems. In Ref. 22, the authors calculated the electric-field induced spin accumulation and spin current in a finite-size sample and showed that the spin Hall conductivity vanishes in an infinite system. Thus, in macroscopic samples, intrinsic SHE vanishes so that in recent years the presence of intrinsic SHE was largely studied in ballistic devices as nanojunctions formed by crossing quasi-one-dimensional (Q1D) devices. In fact, in Ref. 23, the authors demonstrated that the flow of a longitudinal unpolarized current through a ballistic two-dimensional electron gas (2DEG) with SOI will induce a nonequilibrium spin accumulation that has opposite signs for the two lateral edges. The discussion was extended with the

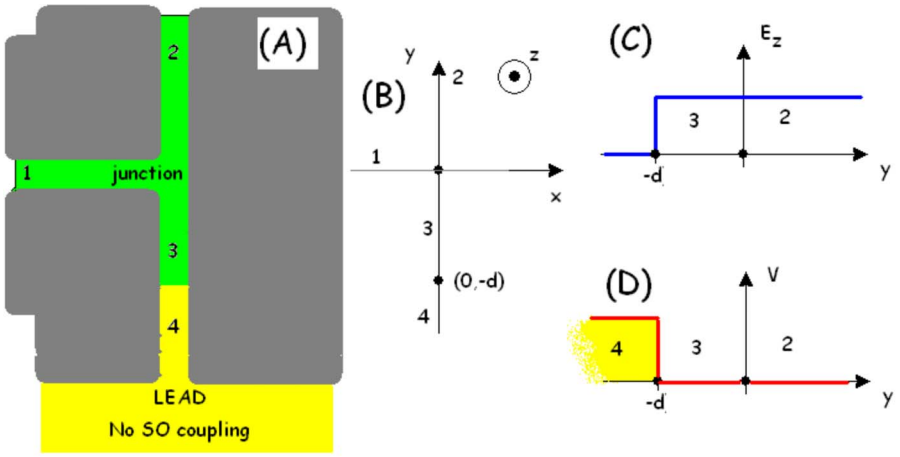

FIG. 1. (Color online) Schematic plots of the T junction (A) with the axis (B) and the shape of the transverse Rashba electric field $E_z(y)$ (C) and potential $V(y)$ (D). The junctions can be assumed as crossing junctions between two Q1D wires of width W ranging between $\sim$25 and 100 nm. We propose a hybrid lead-wire system [a semi-infinite wire ($y>-d$) is attached to an ideal lead ($y<-d$)]. In the wire (sections I–III) a strong Rashba SOI is present, while the latter vanishes in the lead (section IV).

investigation of the SHE in multiprobe ballistic SO coupled semiconductor bridges,[24] i.e., a device where longitudinal leads are attached to ballistic quantum-coherent 2DEG in a semiconductor heterostructure.[23,24] The latter device can be assumed as a crossing junction between two Q1D wires.[25]

Here, we consider low-dimensional electron systems formed by Q1D nanojunctions patterned in a 2DEG where a natural SOI is present, the Rashba coupling, which stems from the structure inversion asymmetry of the heterostructure quantum well. We propose a hybrid lead-junction system, i.e., two crossing semi-infinite wires [section 1 and sections II and III in Fig. 1(a)] with strong Rashba coupling attached to an ideal lead ($y<-d$) where SOI vanishes.

In this paper, we predict that a spin-polarized current can be induced in probe 2 by injecting an unpolarized charge current through probe 1 when the ideal lead 4 does not accept any current. The magnitude of the spin polarization will strongly depend on (i) the distance d between the center of the junction and the ideal lead and (ii) the strength of the SO coupling, arising from the electric field along the z axis (which can be tuned by the gate electrode) that confines electrons within the xy plane of the quantum well in the semiconductor heterostructure. We also predict that a nonequilibrium spin accumulation will appear in the ideal lead 4 to generate a compensating current in the direction opposite to the spin current.

Next, we discuss what happens when the ideal lead 4 can accept a current, and we predict that when an unpolarized charge current is injected through probe 1, (i) a zero bias charge current (pseudo-Hall current) can flow from probe 4 to 2, (ii) a spin-polarized current can be induced from probe 4 to 2, and (iii) tuning the distance d or the strength of the SOI, it is possible to have a pure spin (Hall) current from probe 4 to 2.

II. MODEL AND THEORETICAL APPROACH

A. Rashba spin-orbit interaction

As already mentioned, the Rashba effect[26] originates from the macroscopic electric field in a semiconductor quantum well (a potential well along the z direction, which is present in semiconductor heterostructures). Due to the band offsets at the interface of two different materials, the electrons are confined by forming a 2DEG (in the xy plane). Since an asymmetric quantum well potential confines the electron gas[27] in some heterostructures the electrons move in an effective electric field E_z along $\hat{z}$, and the Hamiltonian in Eq. (1) will take the form[28]

$$\hat{H}_{SO}^{\alpha} = \frac{\alpha}{\hbar}[\sigma_x \mathbf{p}_y - \sigma_y \mathbf{p}_x]. \tag{2}$$

α, which in vacuum is given by $\lambda_0^2 E_z e$, in semiconductor heterostructures takes values typically[29–32] within the range of $\sim 10^{-11}-10^{-12}$ eV m, while its highest value is close to 10^{-10} eV m, as reported in Refs. 33 and 34. In the reference system of the electron, this electrical field transforms into an effective magnetic field. Even though the Rashba spin splitting is expected to be very small, nonetheless, this perturbation can give rise to a sizeable modification of a semiconductor band structure.[29,35] Moreover, for applications, it is essential that the strength of the Rashba effect, and thus the spin splitting, can be controlled by means of a gate electrode.

B. Quantum wave functions

The ballistic one-dimensional wire is a nanometric solid-state device in which the transverse motion (along y for probe 1 in Fig. 1 and along x for wire 2-3-4) is quantized into discrete modes, and the longitudinal motion (y direction for probe 1 in Fig. 1) is free. In this case, electrons propagate freely down to a clean narrow pipe, and electronic transport with no scattering can occur.

Next, we assume that the SO interaction vanishes in sector 4, while in the other sections the Hamiltonian $\hat{H}_{SO}$ is given by the term in Eq. (2).

Here, we discuss the case of a quantum well (QW) oriented along the y axis, in the presence of SO interaction. Following Ref. 36, the lateral confining potential of a QW, $V_c(x)$, is approximated by a parabola,

$$\hat{H}_0 = \frac{\mathbf{p}^2}{2m^*} + V_c(\mathbf{r}) = \frac{\mathbf{p}^2}{2m^*} + \frac{m^*}{2}\omega^2 x^2. \tag{3}$$

The quantity ω controls the curvature of the confining potential.

As we know from Refs. 37 and 38, the QW Hamiltonian in the presence of α-SOC cannot be exactly diagonalized. We can calculate its spectrum (and related wave functions) by a numerical calculation or with simple perturbation theory. In order to get to our result, we analyze the Hamiltonian [Eq. (2)] in the general case and separate the commuting part ($[\hat{H}_c, \hat{H}_0]=0$),

$$\hat{H}_c = \frac{\alpha}{\hbar} p_y \hat{\sigma}_x = \frac{\hbar^2 k_R p_y}{m^*} \hat{\sigma}_x, \tag{4}$$

where $k_R \equiv \frac{m^*\alpha}{\hbar^2}$, which has a natural value[28,39] for $\alpha \sim 10^{-12}$–10^{-10} eV m and $k_R \sim 10^{-5}$–10^{-2} nm^{-1}.

The nondiagonal term

$$\hat{H}_n = \frac{\alpha}{\hbar} p_x \hat{\sigma}_y = \frac{\hbar^2 k_R}{m^* l_\omega} (\hat{a}_x - \hat{a}_x^\dagger)(\hat{\sigma}_+^x + \hat{\sigma}_-^x), \tag{5}$$

where $l_\omega = (\hbar/m^*\omega)^{1/2}$ and $\hat{a}_x, \hat{a}_x^\dagger$ are creation-annihilation operators of the 1D quantum mechanical harmonic oscillator,[40] can be neglected in the first order approximation and becomes relevant just near the crossing points $\pm k_c$,[41] as it was discussed in Refs. 37 and 38 and in bibliography therein.

It follows that the Rashba subband splitting in the energies, in the first order approximation, read

$$\varepsilon_{n,k,s_x} = \hbar\omega\left(n + \frac{1}{2}\right) + \frac{\hbar^2}{2m^*}[(k \pm k_R)^2 - k_R^2]. \tag{6}$$

The $\pm$ sign corresponds to the spin polarization along the x axis, i.e., to the spin eigenstate χ_{s_x} (see the Appendix). Hence, we can conclude that four-split channels are present for a fixed Fermi energy ε_F corresponding to $\pm p_y$ and $s_x = \pm 1$ with eigenfunctions

$$\varphi_{\varepsilon_F,n,s_x} = u_n(x) e^{ik_n^s(\varepsilon_F)y} \chi_{s_x},$$

where $u_n(x)$ are displaced harmonic oscillator eigenfunctions.

Here,

$$k_n^s(\varepsilon_F) = sk_R \pm \sqrt{k_R^2 + k_n^2} \equiv sk_R \pm q_n,$$

where $k_n^2 = \frac{2m^*}{\hbar}(\varepsilon_F - \hbar\omega_T \frac{2n+1}{2})$ and $q_n = \sqrt{k_R^2 + k_n^2}$.

In each of the sectors of the junction, H^α has eigenfunctions belonging to the 1D subbands ($n=0,1,\ldots$). If we suppose that the QWs are quite narrow (1D limit), we can limit ourselves to $n=0$ and neglect the transverse part of the wave function $u_n(x)$.

This approximation can be justified by assuming the energy $\tilde{\varepsilon}_k \equiv \varepsilon_F - \hbar\omega/2$ to be less than $\hbar\omega$ that is $\sim$50 meV for a QW of effective width $W \sim 20$ nm.

Thus, the wave functions in sectors 1, 2, and 3 are built starting from

$$f_{q,\rightarrow}^{\parallel} = e^{iqy} e^{ik_R y} \chi_{\rightarrow}^x, \quad f_{q,\leftarrow}^{\parallel} = e^{iqy} e^{-ik_R y} \chi_{\leftarrow}^x,$$

$$f_{q,\uparrow}^{=} = e^{iqx} e^{ik_R x} \chi_{\uparrow}^y, \quad f_{q,\downarrow}^{=} = e^{iqx} e^{-ik_R x} \chi_{\downarrow}^y,$$

where $\parallel$ stands for probe 2 or 3 and $=$ for sector 1.

In sector 4 where no SO interaction is present, the wave functions are built starting from

$$f_{\kappa,\rightarrow}^{\parallel} = e^{-i\kappa y} \chi_{\rightarrow}^x, \quad f_{\kappa,\leftarrow}^{\parallel} = e^{-i\kappa y} \chi_{\leftarrow}^x,$$

where

$$\kappa_n^s(\varepsilon_F) = \sqrt{\frac{2m^*}{\hbar^2}\left(\varepsilon_F - \hbar\omega_T \frac{2n+1}{2} - V_0\right)},$$

where V_0 is the barrier potential shown in Fig. 1(d).

C. Ballistic transport and Landauer formula

In order to study the transport properties of the system subject to a constant low bias voltage (linear regime), we calculate the zero temperature conductance G based on the Landauer formula,[42]

$$G = \frac{e^2}{h} \sum_{n',n=0}^{M} \sum_{\sigma',\sigma} T_{n'n}^{\sigma'\sigma}, \tag{7}$$

where $T_{n'n}^{\sigma'\sigma}$ denotes the quantum probability of transmission between incoming (n,σ) and outgoing (n',σ') asymptotic states defined on semi-infinite ballistic leads. The labels n,n' and σ,σ' refer to the corresponding mode and spin quantum numbers, respectively. As we have discussed above, we also limit our analysis to the case of just one mode involved: $n=n'=0$.

The Landauer formula works in the ballistic transport regime, in which the dimensions of the sample are reduced below the mean free path of the electrons. Thus, the Landauer formula in the form of Eq. (7) properly works just at $T=0$, while a more general formulation at finite temperatures has to take into account the width of the distribution of injected electrons. Thus, in order to generalize the calculations at finite temperature, the conductance at finite T can be obtained by[43]

$$G = -(e^2/h) \sum_\sigma \int_0^\infty d\varepsilon \frac{\partial F(\varepsilon, \varepsilon_F, T)}{\partial \varepsilon} |T_\sigma(\varepsilon_F)|^2, \tag{8}$$

where F is the Fermi distribution function and T the temperature.

D. Theoretical treatment of the scattering

We approach this scattering problem using the quantum waveguide theory[44] justified for strictly one-dimensional devices. The incident wave can be taken in probe 1 with spin $S_y = \pm\hbar/2$ as

$$\psi_{0\uparrow}^1 = e^{i(q+k_R)x} \chi_\uparrow, \quad \psi_{0\downarrow}^1 = e^{i(q-k_R)x} \chi_\downarrow.$$

Next, we use the Griffith boundary condition,[45] which states that the wave function is continuous and that the current density is conserved at each intersection $[(0,0),(0,-\mathrm{d})]$. The resulting set of linear equations [Eq. (A1)] leads to a relation between the expansion coefficients t_q^s in the different do-

mains (see the Appendix). Thus, the transmission problem can be solved exactly by matching appropriate *Ansätze* for wave functions in the wires. Then, we obtain the transmission coefficients $T_{pq}^{s,\sigma}$, where s is the spin of the injected electron in probe p and σ is the spin of the exiting one in probe q. Here, s and σ can be $\uparrow$, $\downarrow$, or $\rightarrow$, $\leftarrow$.

III. RESULTS

Since the SO coupling often vanishes in the contacts,[37,38] it can be useful to analyze the behavior of a hybrid system. In the latter system, the transport is strongly affected by the scattering at junction-lead interfaces due to the different nature of electron states in the wires and the lead. The simplest model[46,47] is the one obtained by attaching semi-infinite leads with $k_R=0$ (section IV corresponding to $y<-d$) to the junction where $k_R \neq 0$.

The first result concerns the symmetry of transmission coefficients $T_{pq}^{s,\sigma}$ as functions of the parameters. We can calculate them analytically, as we report in the Appendix [Eqs. (A2) and (A3)]. We first focus on probe 2. It follows that

$$T_{12}^{s_y,\rightarrow} = \tau(2qd + \varphi_R), \quad T_{12}^{s_y,\leftarrow} = \tau(2qd - \varphi_R),$$

where τ is a simple function, and the phase shift reads $\varphi_R = 2k_R d$. Thus, the symmetry breaking between spin$\leftarrow$ and spin$\rightarrow$electrons is clearly induced by the quantum interference in the region $0>y>-d$. This polarization is present if we inject both a spin unpolarized current and a polarized one in probe 1.

A. Lead 2 conductance

Here, we suppose that the potential of the ideal lead (V_0) is much larger than the energy $\tilde{\varepsilon}_K$ of the injected electrons in probe 1. Since no current flows through probe 4, the device is reduced to a two-terminal one, i.e., the current injected in lead 1 (source) can just exit from probe 2 (drain).

By a comparison between the transmission amplitudes, it is evident that a spin-polarized current can be generated in lead 2 and can be modulated by acting on the parameter φ_R. In order to see this modulation clearly, we introduce a dimensionless quantity P_x to describe the spin polarization along the x axis of current transmitted in lead 2, which is defined by

$$P_x(\varepsilon_F, \varphi_R) = \frac{j_\rightarrow - j_\leftarrow}{j_\rightarrow + j_\leftarrow} = \frac{T_{12}^{\uparrow,\rightarrow} + T_{12}^{\downarrow,\rightarrow} - T_{12}^{\uparrow,\leftarrow} - T_{12}^{\downarrow,\leftarrow}}{T_{12}^{\uparrow,\rightarrow} + T_{12}^{\downarrow,\rightarrow} + T_{12}^{\uparrow,\leftarrow} + T_{12}^{\downarrow,\leftarrow}},$$

where the spin resolved currents j_s were obtained by employing the Landauer formula. Here, P_x is similar to the spin injection rate defined in ferromagnetic/semiconductor/ferromagnetic heterostructures,[48] and it can be measured experimentally.[49]

As we show in Fig. 2, where P_x is reported as a function of d and $\tilde{\varepsilon}_K$, we predict that a spin-polarized current can be induced in probe 2 by injecting an unpolarized charge current through probe 1 when the ideal lead 4 does not accept any current. The magnitude of the spin polarization will strongly depend both on the distance d between the center of the junction and the ideal lead and on the strength of the SOI.

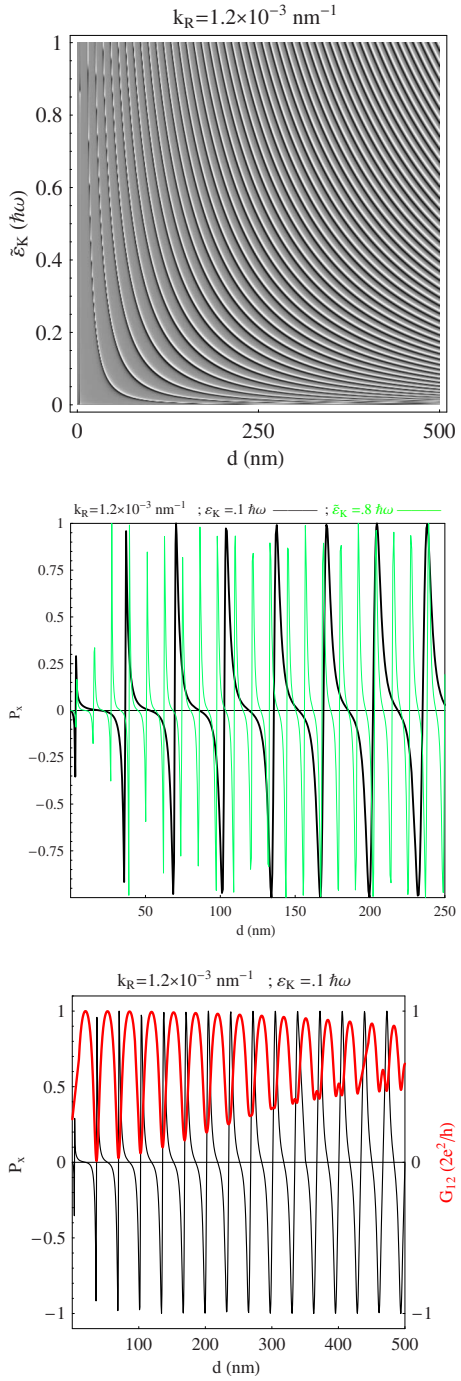

FIG. 2. (Color online) Spin polarization of the emerging current in lead 2. Here, $V_0 \sim 2\hbar\omega$ (we suppose $\hbar\omega \sim 50$ meV) and $k_R = 1.2 \times 10^{-3}$ nm^{-1}. (Top) Density plot of the spin polarization as a function of the cavity length and the kinetic energy $\tilde{\varepsilon}_K$ from 0 to the bottom of the second subband. (Bottom left) The oscillation for two fixed values $\tilde{\varepsilon}_K \sim 0.1\hbar\omega$ (black thick line) and $\tilde{\varepsilon}_K \sim 0.8\hbar\omega$. (Bottom right) The charge conductance (G_{12}, thick line) compared to the spin polarization (black thin line) as a function of d.

This dependence produces the oscillations shown in Fig. 2.

We can also observe that the maxima of the spin polarization correspond to the minima of the charge conductance (obtained by applying the two-terminal Landauer formula),

which, however, is significantly nonvanishing for large d.

Also, if no current can flow in probe 4, a nonequilibrium spin accumulation will appear in the ideal lead 4 in order to generate a compensating current in the direction opposite to the spin current. In general, the quantum interference in the region $0<y<-d$ can produce a spin-polarized current by deflecting opposite spin electrons in opposite directions, yielding a spin accumulation $\langle S_x\rangle$ in the probes (2 and 4). Obviously, this spin polarization corresponds to a current that flows in probe 2, while in the lead the spin polarization disappears at a distance from the interface of some $\ell_V = 1/(i\kappa)$ corresponding to a few tens of nanometers.

In Fig. 3, we show the spin accumulation $\langle S_x\rangle$ as a function of k_R and $\tilde{\varepsilon}_K$, both in leads 2 and 4.

B. Three probe conductance

Next, we discuss what happens when the ideal lead 4 can accept a current. Here, we assume that V_0 vanishes, so that the only difference between the junction and the lead consists in the absence of SOI. Thus, we can now define the spin polarization for the currents I_2 and I_4 in the top and bottom probes. We can observe that the SOI and the quantum interference can give currents with opposite spin polarization flowing in the opposite probes, as shown in Fig. 4.

The correspondence between this spin polarization and the presence of a transverse spin Hall current can now be discussed, starting from a theory for the quantum transport of spin currents in a three-terminal device. In fact, the current can now flow out of the junction also by probe 4. The charge currents in mesoscopic structures attached to many leads are described by the Landauer-Büttiker formulas,[50] which generalize the Landauer formula for two-terminal devices to a multiprobe system,

$$I_p = \sum_{q\neq p} G_{pq}(V_p - V_q), \tag{9}$$

while the analogous formulas for the spin currents in the leads are straightforwardly extracted from them,[51,52]

$$I_p^s = \frac{\hbar}{2e}\sum_{q\neq p} (G_{qp}^{\text{out}} V_p - G_{pq}^{\text{in}} V_q), \tag{10}$$

where $G_{pq}^{\text{in}} = G_{pq}^{\uparrow\uparrow} + G_{pq}^{\uparrow\downarrow} - G_{pq}^{\downarrow\uparrow} - G_{pq}^{\downarrow\downarrow}$ and $G_{qp}^{\text{out}} = G_{qp}^{\uparrow\uparrow} + G_{qp}^{\downarrow\uparrow} - G_{qp}^{\uparrow\downarrow} - G_{qp}^{\downarrow\downarrow}$.

The conductance coefficients are related to the transmission matrices $\mathbf{t}^{pq}$ between leads p and q through the Landauer-type formula $G_{pq}^{\alpha\alpha'} = \frac{e^2}{h}\Sigma_{i,j=1}^{M_{\text{leads}}} |\mathbf{t}_{ij,\alpha\alpha'}^{pq}|^2$, where $|\mathbf{t}_{ij,\alpha\alpha'}^{pq}|^2$ is the probability for spin-α' electron incident in lead q to be transmitted to lead p as a spin-α electron and i,j label the transverse propagating modes (i.e., conducting channels) in the leads.

Now, we fix the potential $V_1 = \Delta\mu$ while $V_2 = V_4 = 0$. The charge current in probe 2 is now given by

$$I_2 = I_2^{\rightarrow} + I_2^{\leftarrow} = \frac{e^2}{\hbar}\Delta\mu([T_{12}^{\uparrow\rightarrow} + T_{12}^{\downarrow\rightarrow}] + [T_{12}^{\uparrow\leftarrow} + T_{12}^{\uparrow\leftarrow}]),$$

while in probe 4 it results to

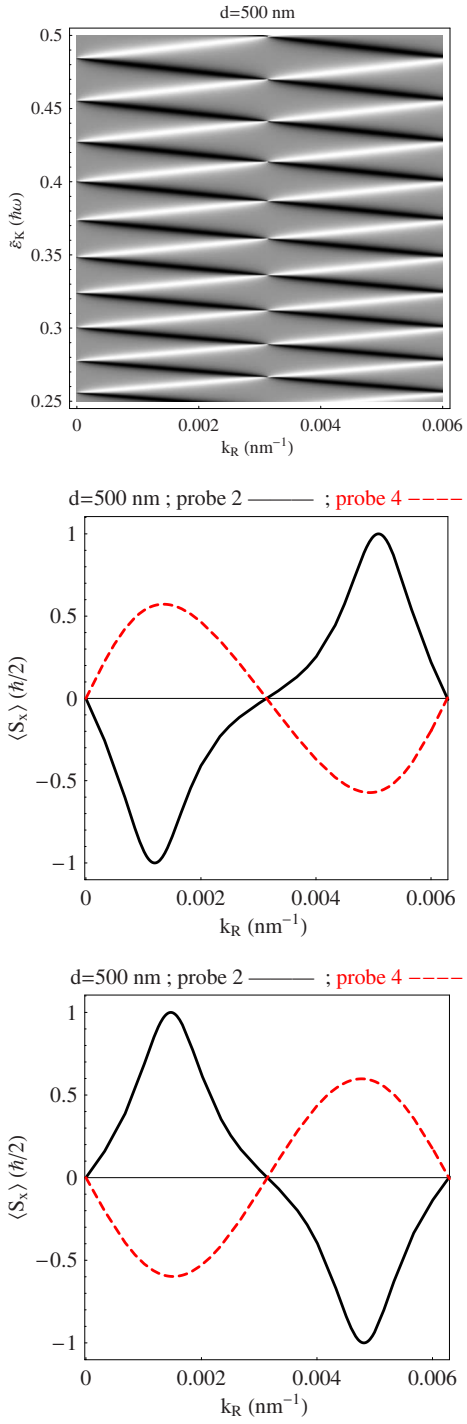

FIG. 3. (Color online) (Top) Spin polarization of the emerging current in lead 2. Here, $V_0 \sim 2\hbar\omega$ (we suppose $\hbar\omega \sim 50$ meV) and $k_R = 1.2\times 10^{-3}$ nm^{-1}. Density plot of the spin polarization as a function of the strength of the SOI, k_R, and the kinetic energy $\tilde{\varepsilon}_K$ from 0 to the bottom of the second subband. (Bottom) The spin accumulation $\langle S_x\rangle$ across the probes (2 and 4) of the ballistic T junction as a function of the SOI strength (k_R). Here, $V_0 \sim 2\hbar\omega$ (we assume $\hbar\omega \sim 50$ meV). We observe that the spin polarizations are opposite each other. (Left) $\varepsilon_K \sim 0.1\hbar\omega$, the penetration length ℓ_V of the spin polarization in probe 4 is ~ 3.5 nm. (Right) $\varepsilon_K \sim 0.8\hbar\omega$, and the penetration length ℓ_V of the spin polarization in probe 4 is ~ 7.3 nm.

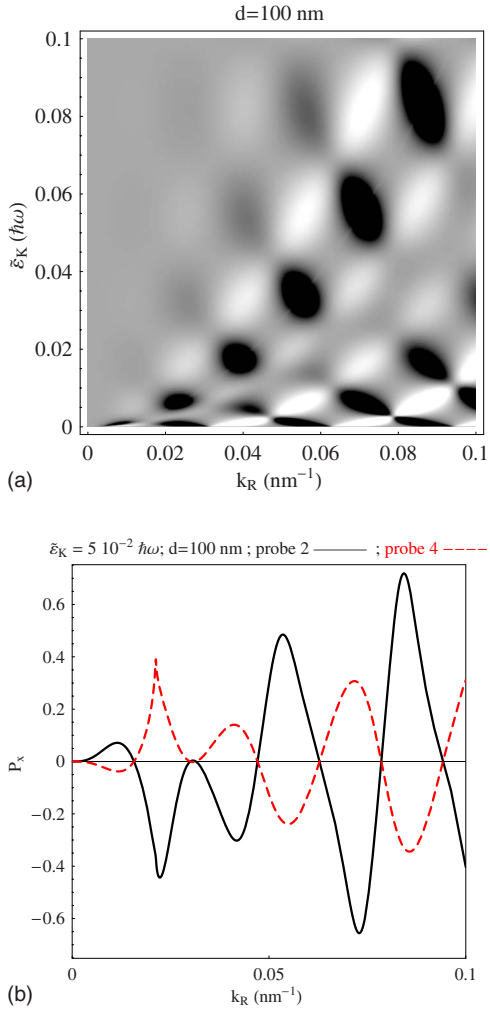

FIG. 4. (Color online) (Top) Spin polarization of the emerging current in lead 2. Here, $V_0=0$ and $d=100$ nm. Density plot of the spin polarization as a function of the strength of the SOI, k_R, and the kinetic energy $\tilde{\varepsilon}_K$. (Bottom) Spin polarization of the emerging current in leads 2 (I_2) and 4 (I_4) versus the the strength of the SOI, k_R for a fixed value of $\tilde{\varepsilon}_K=510^{-3}\hbar\omega$ (if we assume $W\sim 50$ nm, and we have $\tilde{\varepsilon}_K\sim 0.25$ meV).

$$I_4 = I_4^{\rightarrow} + I_4^{\leftarrow} = \frac{e^2}{\hbar}\Delta\mu([T_{14}^{\uparrow\rightarrow} + T_{14}^{\downarrow\rightarrow}] + [T_{14}^{\uparrow\leftarrow} + T_{14}^{\uparrow\leftarrow}]).$$

We can define a "pseudo-Hall" current as the current that flows between probes 2 and 4 without any bias voltage,

$$I_H = I_2 - I_4,$$

and it does not vanish because of the spin induced symmetry breaking (as we show in Fig. 5, bright line).

This current is also spin polarized as we can calculate. The "pseudo-spin-Hall current" is obtained from the Buttiker-Landauer theory as

$$I_{sH} = I_2^{\rightarrow} - I_2^{\leftarrow} - I_4^{\rightarrow} + I_4^{\leftarrow}.$$

In Fig. 5, we show a comparison between charge and spin transverse currents between probes 2 and 4. It follows that we could modulate the angle φ_R (e.g., the strength of the Rashba coupling) in order to obtain a spin unpolarized transverse current or a pure spin current. In the latter cases, it follows that to a charge current I_0 injected in lead 1 corresponds a transverse SH current given by the equation above; i.e., the spin accumulation will push the pure spin current I_{sH} into the transverse probes.

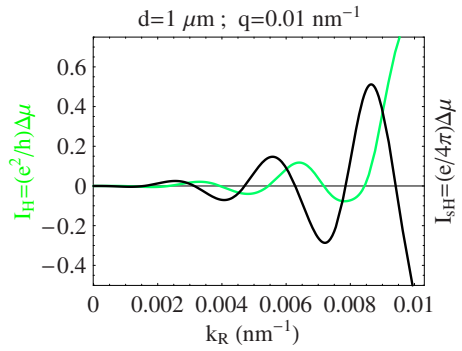

FIG. 5. (Color online) Charge and spin transverse currents between probes 2 and 4. We can observe that for $k_R\sim 0.007$, the spin current vanishes and a pure charge current flows from lead 2 to lead 4. For $k_R\sim 0.0065$, the charge current vanishes and a *pure spin current* flows from probe 4 to probe 2.

Notice that for vanishing d, the symmetry breaking disappears because the main role in the spin polarization and transverse current generation is played by the quantum interference. The symmetry breaking is due to the interplay between quantum interference and spin-orbit interaction. However, according the discussion of Ref. 23, in many cases the detection of the currents requires one to measure the spin accumulation that they deposit at the sample edges.[53]

IV. DISCUSSION

In this paper, we discussed some theoretical devices capable of acting as spin filters based on the Rashba interaction. Now, we can summarize our results by starting from the feasibility of similar devices.

The first question concerns the SOI strengths. The values of α have been theoretically evaluated for some semiconductor compounds.[54] In a QW patterned in InGaAs/InP heterostructures, λ^2 takes values between 50 and 150 Å^2; hence, in the usual devices,[28,39] the natural values read $\alpha\sim 10^{-11}$ eV m and $k_R\sim 10^{-4}$ nm^{-1}. For GaAs heterostructures, λ^2 is one order of magnitude smaller ($\sim$4.4 Å^2) than in InGaAs/InP, whereas for HgTe based heterostructures, it can be more than three times larger.[55] Thus, values of k_R up to $\sim 10^{-2}$ nm^{-1} can be assumed due to the natural SOI, i.e., to the structure inversion asymmetry of the heterostructure quantum well. On the contrary, larger values (as those used in Fig. 4) have to be obtained by controlling the transverse electric field, e.g., by tuning the voltage on the gate electrode.

The second question concerns the size of the discussed devices. A typical nanojunction should be made by using narrow QWs of a width W from tens to hundreds of nanometers. In fact, the lithographical width of a wire defined in a

2DEG can be as small as 20 nm,[56] always away from the saturation region. Moreover, we have to fix d of the order of some hundreds of nanometers, i.e., distances surely available with a good precision.

The device proposed here can be compared to the one in Ref. 23 where the value of α can take values that correspond to $k_R \sim 5 \times 10^{-2}$ nm^{-1}, while W is $\sim$25 nm. There was a predicted spin accumulation $\langle S_z \rangle$ that ranges from $10^{-4}\hbar/2$ to $10^{-3}\hbar/2$.

In this paper, we proposed a scheme of spin filtering based on nanometric cross junctions in the presence of Rashba SOI. The cross geometry seems to be one of the most efficient devices for the spin filtering because it acts like a kind of ultrasensitive scale, capable of reacting to the smallest variations of external or effective fields. In this paper, we take into account a hybrid lead-junction system, i.e., a cross junction with strong Rashba coupling attached to an ideal lead where the SOI vanishes. Due to the quantum interference in the cavity between the center of the cross junction and the ideal lead, there is a symmetry breaking between currents with opposite spin polarization. Thus, tuning the distance d or the strength of the SOI, it is possible to modulate the interferometric phase φ_R.

Here, we discussed two different cases. The first device that we proposed is a two-terminal device attached to the interferometer discussed above. In fact, no current can flow through the ideal lead. We showed that a spin-polarized current can be induced in probe 2 by injecting an unpolarized charge current through probe 1, while just a nonequilibrium spin accumulation will appear in the ideal lead 4. The second case corresponds to a three terminal T junction. Here, we showed that when an unpolarized charge current is injected through probe 1, (i) a zero bias charge current (pseudo-Hall current) can flow from probe 4 to 2, (ii) a spin-polarized current can be induced from probe 4 to 2, and (iii) a pure spin (Hall) current can go from probe 4 to 2.

The effects of spin interference caused by Rashba SOI were largely studied in the past years and, more recently, they were measured experimentally. In Ref. 57, the authors studied Aharonov-Bohm-type conductance oscillations in ring structures fabricated from HgTe=HgCdTe as a function of Rashba SOI strength and associated these observations with the Aharonov-Casher (AC) effect. More recently, the AC effect was demonstrated also in small arrays of mesoscopic semiconductor rings.[58] The AC oscillations were also discussed in Ref. 59 where a Rashba gate controlled ring embedded in a p-type self-assembled silicon quantum well was analyzed. This analysis was developed also for a three-terminal device with a quantum dot[60] or a quantum point contact (QPC)[61] inserted in one of the ring's arms using the split-gate technique.[62] This device can be appropriate in order to divide the relative contribution of the AC effect in the conductance oscillations. The presence of a nonmagnetic obstacle as a QPC was also analyzed in our recent paper[63] where we demonstrated the central role that it plays in inducing a significant spin polarization in the current flowing in a two-terminal quantum ring.

Thus, the idea to use two and three-terminal interferometric devices as spin filters is not new. However, most of the proposals are based on a ring geometry.[64,65] This geometry was required in order to optimize the spin filtering of the simple T stub proposed in Ref. 66 where no interferometric effects are present. From an experimental point of view, the latter device requires the presence of a localized SOI formed in the 2D electron gas layer by gate electrodes and localized to the area of intersection only.

The devices proposed in this paper are linear interferometers that present two kinds of advantages with respect to the earlier proposals mentioned above. From a technological point of view, one advantage is due to the linear, rather than circular, geometry that gives more compactness to the device and a higher readiness and easiness in manufacturing it, which could be relevant when planning a spintronic circuit made of several such elements. The possibility of acting on different parameters, such as the interferometric distance d, allows one for a better control on the required phase.

From a theoretical point of view, our device is based on a simpler interferometric effect than the ones based on the ring geometry. In fact, the presence of a ring in the interferometer introduce an extra phase due to the curvature of the channel, which can be associated with the Berry phase.

Moreover, the two terminal interferometer proposed above can be optimized by acting on parameters (Fig. 2) in order to obtain a higher spin polarization and a significant current (high transmission), while the same device allows the measurement of the spin accumulation in region 4.

ACKNOWLEDGMENT

We acknowledge the support of the 2006 PRIN grant "Sistemi Quantistici Macroscopici-Aspetti Fondamentali ed Applicazioni di strutture Josephson Non Convenzionali."

APPENDIX: USEFUL FORMULAS

Let us introduce the three spin operators $\hat{\sigma}_i$ in the x-based representation,

$$\hat{\sigma}_x = \frac{\hbar}{2}\begin{pmatrix} 1 & 0 \\ 0 & -1 \end{pmatrix}, \quad \hat{\sigma}_y = \frac{\hbar}{2}\begin{pmatrix} 0 & 1 \\ 1 & 0 \end{pmatrix}, \quad \hat{\sigma}_z = \frac{\hbar}{2}\begin{pmatrix} 0 & i \\ -i & 0 \end{pmatrix}.$$

Next, we assume for an electron with spin $s_x = \pm 1$ ($S_x = \pm \hbar/2$) corresponding to the spinor,

$$\chi_{\rightarrow} \equiv \begin{pmatrix} 1 \\ 0 \end{pmatrix}, \quad \chi_{\leftarrow} \equiv \begin{pmatrix} 0 \\ 1 \end{pmatrix},$$

while for an electron with spin $s_y = \pm 1$,

$$\chi_{\uparrow} \equiv \frac{1}{\sqrt{2}}\begin{pmatrix} 1 \\ 1 \end{pmatrix}, \quad \chi_{\rightarrow} \equiv \frac{1}{\sqrt{2}}\begin{pmatrix} 1 \\ -1 \end{pmatrix}.$$

It follows that the wave functions in different regions for each value of the spin are given below,

$$\psi_1 = t_1^{\uparrow} e^{-i(q-k_R)x}\chi_{\uparrow} + t_1^{\downarrow} e^{-i(q+k_R)x}\chi_{\downarrow},$$

$$\psi_2 = t_2^{\rightarrow} e^{-i(q+k_R)y}\chi_{\rightarrow} + t_2^{\leftarrow} e^{-i(q-k_R)y}\chi_{\leftarrow},$$

$$\psi_{(3)} = A^{\rightarrow} e^{i(q+k_R)y}\chi_{\rightarrow} + B^{\rightarrow} e^{-i(q-k_R)y}\chi_{\rightarrow} + A^{\leftarrow} e^{i(q-k_R)y}\chi_{\leftarrow} + B^{\leftarrow} e^{-i(q+k_R)y}\chi_{\leftarrow},$$

$$\psi_4 = t_4^{\rightarrow} e^{-i(\kappa)y}\chi_{\rightarrow} + t_4^{\leftarrow} e^{-i(\kappa)y}\chi_{\leftarrow}. \tag{A1}$$

1. Transmission elements

First, we focus on the transmission elements between probes 1 and 2,

$$t_{12}^{\uparrow\rightarrow} = t_{12}^{\downarrow\rightarrow} = \frac{q\cos[(q+k_R)2d] + i\kappa\sin[(q+k_R)2d]}{D_+}, \tag{A2}$$

$$t_{12}^{\uparrow\leftarrow} = t_{12}^{\downarrow\leftarrow} = \frac{q\cos[(q-k_R)2d] + i\kappa\sin[(q-k_R)2d]}{D_-}, \tag{A3}$$

where

$$D_{\pm} = \frac{1}{\sqrt{2}}(3(q-\kappa) + (q+\kappa)e^{i(q\pm k_R)2d}).$$

It is now clear that if $\kappa=q$, the transmission is reduced to the one of a simple T junction without any spin polarization and dependence on the Fermi energy.

In order to focus on the role that the interference plays in this device, we can analyze the limit $d=0$. In fact, in the latter case, the transmission reads

$$|t_{12}^{s,\sigma}|^2 = \left|\frac{\sqrt{2}q}{4q-2\kappa}\right|^2,$$

without any difference between spin-up and spin-down electrons. A similar result can be obtained for $k_R=0$, where the interference modulates the charge conductance but cannot have any effect on the spin polarization of the current. In fact, we have

$$t_{12}^{\uparrow\rightarrow} = t_{12}^{\downarrow\rightarrow} = t_{12}^{\uparrow\leftarrow} = t_{12}^{\downarrow\leftarrow}.$$

We can also calculate the transmissions amplitudes in probe 4, obtaining

$$t_{14}^{\uparrow\rightarrow} = t_{14}^{\downarrow\rightarrow} = \frac{2\sqrt{2}e^{i\kappa d}}{D_+}, \tag{A4}$$

$$t_{14}^{\uparrow\leftarrow} = -t_{14}^{\downarrow\leftarrow} = \frac{2\sqrt{2}e^{i\kappa d}}{D_-}. \tag{A5}$$

[1] D. D. Awschalom, D. Loss, and N. Samarth, *Semiconductor Spintronics and Quantum Computation* (Springer, Berlin, 2002); B. E. Kane, Nature (London) **393**, 133 (1998).
[2] S. A. Wolf, D. D. Awschalom, R. A. Buhrman, J. M. Daughton, S. von Molnar, M. L. Roukes, A. Y. Chtchelkanova, and D. M. Treger, Science **294**, 1488 (2001).
[3] L. D. Landau and E. M. Lifshitz, *Quantum Mechanics* (Pergamon, Oxford, 1991).
[4] M. A. M. Gijs and G. E. W. Bauer, Adv. Phys. **46**, 285 (1997).
[5] F. Meier and D. Loss, Phys. Rev. Lett. **90**, 167204 (2003).
[6] M. I. D'yakonov and V. I. Perel', JETP Lett. **13**, 467 (1971).
[7] J. E. Hirsch, Phys. Rev. Lett. **83**, 1834 (1999).
[8] D. Culcer, J. Sinova, N. A. Sinitsyn, T. Jungwirth, A. H. MacDonald, and Q. Niu, Phys. Rev. Lett. **93**, 046602 (2004).
[9] S. Bellucci and P. Onorato, Phys. Rev. B **73**, 045329 (2006).
[10] *The Hall Effect and Its Applications*, edited by C. L. Chien and C. W. Westgate (Plenum, New York, 1980).
[11] P. Noziéres and C. Lewiner, J. Phys. (Paris) **34**, 901 (1973).
[12] J. Smit, Physica (Amsterdam) **21**, 877 (1955).
[13] J. Smit, Physica (Amsterdam) **24**, 39 (1958).
[14] N. F. Mott and H. S. W. Massey, *The Theory of Atomic Collisions* (Oxford University Press, New York, 1964).
[15] L. Berger, Phys. Rev. B **2**, 4559 (1970).
[16] L. Berger, Phys. Rev. B **5**, 1862 (1972).
[17] S. K. Lyo and T. Holstein, Phys. Rev. Lett. **29**, 423 (1972).
[18] E. M. Hankiewicz and G. Vignale, Phys. Rev. B **73**, 115339 (2006).
[19] S. Murakami, N. Nagaosa, and S. C. Zhang, Science **301**, 1348 (2003).
[20] J. Sinova, D. Culcer, Q. Niu, N. A. Sinitsyn, T. Jungwirth, and A. H. MacDonald, Phys. Rev. Lett. **92**, 126603 (2004).
[21] L. Sheng, D. N. Sheng, and C. S. Ting, Phys. Rev. Lett. **94**, 016602 (2005); E. M. Hankiewicz, L. W. Molenkamp, T. Jungwirth, and J. Sinova, Phys. Rev. B **70**, 241301(R) (2004).
[22] E. G. Mishchenko, A. V. Shytov, and B. I. Halperin, Phys. Rev. Lett. **93**, 226602 (2004).
[23] B. K. Nikolic, S. Souma, L. P. Zarbo, and J. Sinova, Phys. Rev. Lett. **95**, 046601 (2005).
[24] B. K. Nikolic, L. P. Zarbo, and S. Souma, Phys. Rev. B **72**, 075361 (2005).
[25] The width W of each Q1D corresponding to the device proposed in Ref. 23 ranges from ~25 to 100 nm.
[26] Y. A. Bychkov and E. Rashba, JETP Lett. **39**, 78 (1984); J. Phys. C **17**, 6039 (1984).
[27] M. J. Kelly, *Low-Dimensional Semiconductors: Material, Physics, Technology, Devices* (Oxford University Press, Oxford, 1995).
[28] A. V. Moroz and C. H. W. Barnes, Phys. Rev. B **61**, R2464 (2000).
[29] J. Nitta, T. Akazaki, H. Takayanagi, and T. Enoki, Phys. Rev. Lett. **78**, 1335 (1997).
[30] B. Das, S. Datta, and R. Reifenberger, Phys. Rev. B **41**, 8278 (1990).
[31] J. Luo, H. Munekata, F. F. Fang, and P. J. Stiles, Phys. Rev. B **41**, 7685 (1990).
[32] T. Hassenkam, S. Pedersen, K. Baklanov, A. Kristensen, C. B. Sorensen, P. E. Lindelof, F. G. Pikus, and G. E. Pikus, Phys. Rev. B **55**, 9298 (1997).
[33] G. Engels, J. Lange, Th. Schäpers, and H. Lüth, Phys. Rev. B **55**, R1958 (1997).
[34] M. Schultz, F. Heinrichs, U. Merkt, T. Colin, T. Skauli, and S. Løvold, Semicond. Sci. Technol. **11**, 1168 (1996).
[35] H. L. Stormer, Z. Schlesinger, A. Chang, D. C. Tsui, A. C. Gossard, and W. Wiegmann, Phys. Rev. Lett. **51**, 126 (1983).

[36] S. E. Laux, D. J. Frank, and F. Stern, Surf. Sci. **196**, 101 (1988); H. Drexler W. Hansen, S. Manus, J. P. Kotthaus, M. Holland, and S. P. Beaumont, Phys. Rev. B **49**, 14074 (1994); B. Kardynal, C. H. W. Barnes, E. H. Linfield, D. A. Ritchie, J. T. Nicholls, K. M. Brown, G. A. C. Jones, and M. Pepper, *ibid.* **55**, R1966 (1997).

[37] M. Governale and U. Zulicke, Phys. Rev. B **66**, 073311 (2002).

[38] S. Bellucci and P. Onorato, Phys. Rev. B **68**, 245322 (2003).

[39] D. Grundler, Phys. Rev. Lett. **84**, 6074 (2000).

[40] A. Messiah, *Quantum Mechanics* (North-Holland, Amsterdam, 1961).

[41] $k_c \equiv \frac{\hbar p_R}{m^* l_\omega (\hbar\omega + 2\hbar^2 k_y k_R / m^*)}$.

[42] R. Landauer, IBM J. Res. Dev. **1**, 233 (1957); R. Landauer, Philos. Mag. **21**, 863 (1970).

[43] R. Citro, F. Romeo, and M. Marinaro, Phys. Rev. B **74**, 115329 (2006).

[44] J. B. Xia, Phys. Rev. B **45**, 3593 (1992); P. S. Deo and A. M. Jayannavar, *ibid.* **50**, 11629 (1994).

[45] S. Griffith, Trans. Faraday Soc. **49**, 345 (1953); **49**, 650 (1953).

[46] F. Mireles and G. Kirczenow, Phys. Rev. B **64**, 024426 (2001).

[47] L. W. Molenkamp, G. Schmidt, and G. E. W. Bauer, Phys. Rev. B **64**, 121202(R) (2001).

[48] M. Johnson, Phys. Rev. B **58**, 9635 (1998); M. Johnson and R. H. Silsbee, *ibid.* **37**, 5326 (1988).

[49] Shun-Qing Shen, Zhi-Jian Li, and Zhongshui Ma, Appl. Phys. Lett. **84**, 996 (2004).

[50] M. Büttiker, Phys. Rev. Lett. **57**, 1761 (1986).

[51] T. P. Pareek, Phys. Rev. Lett. **92**, 076601 (2004).

[52] B. K. Nikolić, L. P. Zârbo, and S. Souma, Phys. Rev. B **72**, 075361 (2005).

[53] Y. K. Kato, R. C. Myers, A. C. Gossard, and D. D. Awschalom, Science **306**, 1910 (2004); J. Wunderlich, B. Kaestner, J. Sinova, and T. Jungwirth, Phys. Rev. Lett. **94**, 047204 (2005).

[54] E. A. de Andrada e Silva, G. C. La Rocca, and F. Bassani, Phys. Rev. B **55**, 16293 (1997).

[55] X. C. Zhang, A. Pfeuffer-Jeschke, K. Ortner, V. Hock, H. Buhmann, C. R. Becker, and G. Landwehr, Phys. Rev. B **63**, 245305 (2001).

[56] M. Knop, M. Richter, R. Maßmann, U. Wieser, U. Kunze, D. Reuter, C. Riedesel, and A. D. Wieck, Semicond. Sci. Technol. **20**, 814 (2005).

[57] M. Konig, T. Tschetschetkin, E. M. Hankiewicz, J. Sinova, V. Hock, V. Daumer, M. Schafer, C. R. Becker, H. Buhmann, and L. W. Molenkamp, Phys. Rev. Lett. **96**, 076804 (2006).

[58] T. Bergsten, T. Kobayashi, Y. Sekine, and J. Nitta, Phys. Rev. Lett. **97**, 196803 (2006).

[59] N. T. Bagraev, N. G. Galkin, W. Gehlhoff, L. E. Klyachkin, A. M. Malyarenko, and I. A. Shelykh, J. Phys.: Condens. Matter **18**, L567 (2006).

[60] R. Schuster, E. Buks, M. Heiblum, D. Mahalu, V. Umansky, and H. Shtrikman, Nature (London) **385**, 417 (1997).

[61] N. T. Bagraev, A. D. Bouravleuv, W. Gehlhoff, V. K. Ivanov, L. E. Klyachkin, A. M. Malyarenko, S. A. Rykov, and I. A. Shelykh, Physica E (Amsterdam) **12**, 762 (2002).

[62] T. J. Thornton, M. Pepper, H. Ahmed, D. Andrews, and G. J. Davies, Phys. Rev. Lett. **56**, 1198 (1986).

[63] S. Bellucci and P. Onorato, J. Phys.: Condens. Matter **19**, 395020 (2007).

[64] A. A. Kiselev and K. W. Kim, J. Appl. Phys. **94**, 4001 (2003).

[65] I. A. Shelykh, N. G. Galkin, and N. T. Bagraev, Phys. Rev. B **72**, 235316 (2005).

[66] A. A. Kiselev and K. W. Kim, Appl. Phys. Lett. **78**, 775 (2001).